Superposition Turbo TCM for Multi-Rate Broadcast

Thomas W. Sun[1], Richard D. Wesel[1], Mark R. Shane[1] and Keith Jarett[2]
[1]Electrical Engineering Dept., University of California, Los Angeles, CA 90095
[2]Boeing Satellite Systems, Inc., El Segundo, CA 90245
Email: {wsun, wesel, shane}@ee.ucla.edu, keith.jarett@boeing.com

***Abstract*— Bergmans and Cover identified the capacity region of the Gaussian degraded broadcast channel, where different receivers observe the transmitted signal with different signal to noise ratios. This paper presents a superposition turbo coding scheme that performs within 1 dB of the capacity region boundary of the degraded broadcast channel at BER of 10^{-5}. Performance is consistent over the entire useful range of the power allocation parameter α.**

Coding for the degraded broadcast channel is equivalent to coding for unequal error protection. Adjusting α changes the transmitter constellation of our encoder, and changes the degree to which error protection is unequal. When α is selected to provide equal error protection, the code is essentially a multilevel code. This multilevel code performs as well as single level turbo trellis-coded-modulation schemes with the advantage of the potential for flexible unequal error protection as α is varied.

Keywords Turbo Coding, Superposition, Time Division, Degraded Broadcast Channel, Trellis Coded Modulation.

I. Introduction

In many applications, different receivers could experience different signal-to-noise ratios (SNRs). For example, in satellite television broadcasting, receivers in rain-fades have very low SNRs, while other receivers under clear sky have high SNRs.

With progressive source coding, the data from the video source encoder is not uniformly important. It is desirable that the most important data be recovered even by receivers with poor receiving conditions (i.e. low SNRs). An unequal error protection (UEP) code provides more protection to more important data, permitting it to be received on channels with lower SNR.

Coding for UEP is identical to coding for the degraded broadcast channel. Consider the Gaussian broadcast channel with one sender transmitting X and two receivers observing Y_1 and Y_2 respectively with

$$Y_1 = X + Z_1 \tag{1}$$
$$Y_2 = X + Z_2 \tag{2}$$

where $Z_1 \sim \mathcal{N}(0, N_1)$ and $Z_2 \sim \mathcal{N}(0, N_2)$ with $N_2 > N_1$. This broadcast channel can be re-characterized as the statistically equivalent "degraded" broadcast channel.

$$Y_1 = X + Z_1 \tag{3}$$
$$Y_2 = Y_1 + Z_2' \tag{4}$$

where $Z_2' \sim \mathcal{N}(0, N_2 - N_1)$.

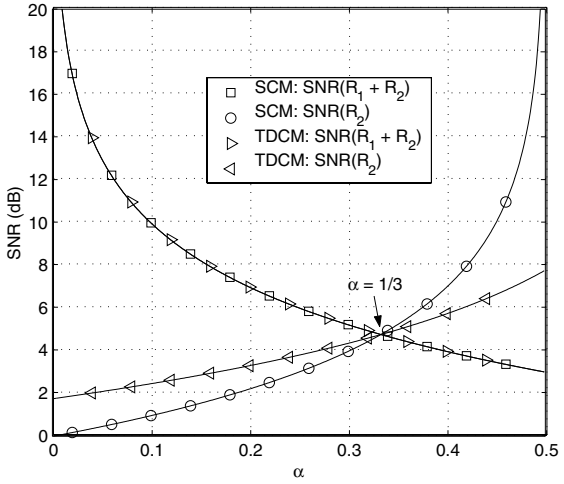

Fig. 1. Comparison of Superposition Coded Modulation (SCM) and Time-Division Coded Modulation (TDCM).

The capacity region for the Gaussian degraded broadcast channel, with signal power constraint P, is given by

$$R_1 < C(\frac{\alpha P}{N_1}) \tag{5}$$
$$R_2 < C(\frac{(1-\alpha)P}{\alpha P + N_2}) \quad \text{for } 0 \le \alpha \le 1 \tag{6}$$

where $C(x) = \log(1 + x)$ denotes the capacity in bits per channel use of a two dimensional memoryless Gaussian channel with SNR x. This region is theoretically achieved by the superposition coding scheme given by Cover in [1]. Bergmans [2], [3] proved the converse. See also [4] for an excellent survey of broadcast channel information theory.

Figure 1 illustrates (5-6) for $R_1 = R_2 = 1$ by plotting the required SNRs for R_2 (circles) and $R_1 + R_2$ (squares) as a function of α. Since (5) assumes that the R_2 data has already been decoded, the plot is meaningful only when the $SNR(R_1+R_2)$ curve lies above the $SNR(R_2)$ curve, i.e. for $\alpha < 1/3$.

Figure 1 shows how α controls the UEP tradeoff. As α decreases, the more important R_2 data can be received at lower and lower SNRs. However, this extra reliability of the R_2 data comes at the cost of decreased reliability for the less important R_1 data which requires a higher and higher SNRs as α decreases.

Figure 1 also shows the performance of an optimal time-division coded modulation (TDCM) scheme designed to match

0-7803-7802-4/03/$17.00 © 2003 IEEE

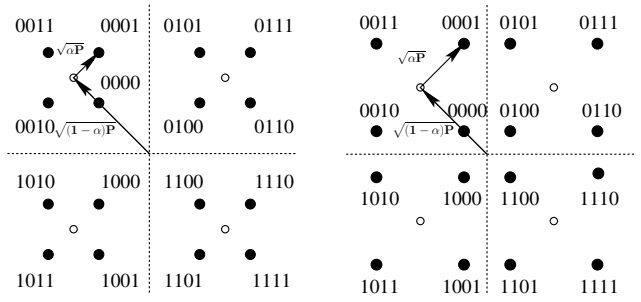

(a) $\alpha = 0.1$ (b) $\alpha = 0.3$

Fig. 2. Example for constellations in simulation for $\alpha = 0.1$, $\alpha = 0.3$

the $R_1 + R_2$ performance of superposition coded modulation (SCM). As shown in the figure, TDCM is theoretically inferior to SCM. However, Wei [5] considered trellis-coded-modulation (TCM) for UEP using both TDCM and SCM approaches, and found TDCM to be superior. Gadkari and Rose [6] explained this behavior by showing that TDCM outperforms SCM for some UEP regions when the channel code performance is sufficiently worse than the capacity-achieving performance assumed in [1], [2], [3]. Recently, Wang and Orchard [7] carefully designed a TCM-based SCM scheme which incorporated shaping. This scheme does outperform TDCM in a UEP region of interest.

In this paper, we use turbo codes to design an SCM. Since turbo codes closely approximate capacity achieving performance, it is not surprising that our SCM closely approach the theoretical SCM curve in Figure 1. In all of our examples, the turbo coded SCM architecture at BER of 10^{-5} performs within 1 dB of the capacity region boundary of the degraded broadcast channel over the entire useful range of the power allocation parameter α.

For our SCM architecture, we use the symbol-interleaved parallel-concatenated turbo TCM (PCTCM) structure of Fragouli and Wesel [8], [9]. The bit-interleaved turbo TCM scheme of Benedetto, Divsalar, and Montorsi [10] is a possible alternative, but bit-interleaving further complicates the initial and subsequent soft information computations. We also implemented SCM using the symbol-interleaved turbo TCM structure of Robertson and Wörz [11], and found its performance to be quite similar to the results presented in this paper, about 0.1 dB worse than SCM based on the Fragouli and Wesel symbol-interleaved architecture.

Section II discusses the power allocation parameter α in detail, and shows that when α takes a certain value, SCM reduces to multi-level coding as discussed in [12]. Section III presents the detail of our SCM turbo TCM architecture. Section IV presents simulation results for two-rate SCMs using 8-point circle constellation and 16-point square constellation as well as a three-rate example using 64-QAM. Section V concludes the paper.

II. Reconfigurability Using α

The α in (5-6) controls the ratio of power allocation to the two data streams. For practical constellations, it decides the Euclidean distances between the constellation points. For a fixed-rate two-rate structure with $R_1 = R_2 = 1$, α can take a value from 0 to 0.5 according to (5-6). However, as shown in Figure 1, with two-stage decoding, only α between 0 and 1/3 makes sense.

When α equals 1/3, the two-rate structure becomes a single rate structure theoretically. It is essentially a multilevel code (MLC), and our two-stage decoding is actually the two-level MLC decoding [12]. By choosing α within $(0, 1/3)$, we configure the system to support two rates with two corresponding operating SNRs.

For standard 16-QAM, the α in (5-6) can be easily determined as 0.2. Solving (5-6) for the maximum N_1 and N_2 with R_1 = R_2 = 1 and $\alpha = 0.2$ yields $N_1 = 0.2P$ and $N_2 = 0.6P$ respectively. The resulting error free SNRs are 7.0 dB and 2.2 dB as shown in Figure 1. Additionally, incorporating the constraint to 16-QAM signaling [13] reduces the tolerable noise to $N_1 = 0.1917P$ and $N_2 = 0.5651P$ respectively. As a result, the error free SNRs are 7.2 dB and 2.5 dB for standard 16-QAM ($\alpha = 0.2$).

Figure 2 shows the 16-point constellations resulting from $\alpha = 0.1$ and $\alpha = 0.3$. Figure 2 also illustrates the edge-profile optimal constellation labeling [14] of the 16-point square constellations used in simulation. It can be seen that the 2 MSB bits of four constellation labelings in the same quadrant are identical.

Figure 2 also shows how α allocates power. For the 16-point square constellation in Figure 2, the 16-point square constellation can be considered as one QPSK constellation added to another QPSK constellation. Two bits of rate-R_2 data are modulated as a QPSK signal which can be mapped to one of four "empty dots" with amplitude of $\sqrt{(1-\alpha)P}$. Then, two bits of rate-R_1 data are modulated as another QPSK signal which can be represented by a solid dot with amplitude of $\sqrt{\alpha P}$, using one of four "empty dots" as its origin.

The following theorem shows that the MLC coding scheme is the special case of multi-rate degraded broadcast channel when all receivers have the same error free SNR. Hence, it is likely we can tune a good MLC code into a good degraded broadcast channel code, or vice versa.

Theorem 1: Consider the Gaussian broadcast channel with one sender and k receivers, $k \geq 1$, we have $Y_i = X + Z_i$, where $Z_i \sim \mathcal{N}(0, N_i)$

$$R_1 < C(\frac{\alpha_1 P}{N_1}), \cdots, \tag{7}$$

$$R_i < C(\frac{\alpha_i P}{\sum_{j=1}^{i-1} \alpha_j P + N_i}), \cdots \tag{8}$$

where $1 \leq i \leq k$, and $\sum_{i=1}^{k} \alpha_i = 1$.

if $N_1 = N_2 = \cdots = N$, then, the rate region reduces to

$$\sum_{i=1}^{k} R_i < C(\frac{P}{N}). \tag{9}$$

Proof: Sum $R_1, \cdots, R_N$ with $N_i = N$. □

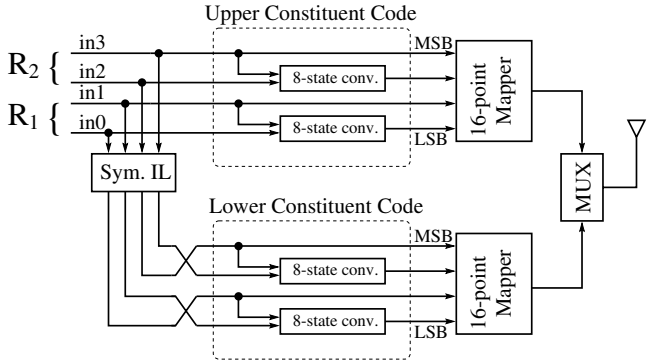

Fig. 3. PCTCM Superposition Turbo TCM Encoder for Two Rates and a 16-point Square Constellation

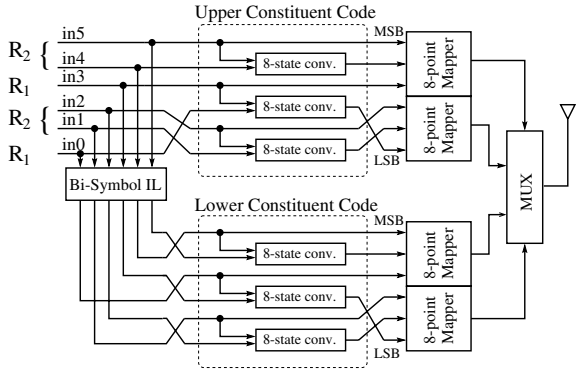

Fig. 4. PCTCM Superposition Turbo TCM Encoder for Two Rates and a 8-point Circular Constellation

This theorem explains why our multi-rate superposition turbo TCM schemes, when configured for single rate, can perform as well as the typical single rate turbo TCM in simulation. If $N_i = N$ and the rates have been fixed to satisfy (9), (7-8) can always be solved for $\alpha_1, \cdots, \alpha_k$. So a good single rate code may be obtained from a good multi-rate code as a special case.

III. The Superposition Turbo TCM

A. Encoder

Figure 3 shows the structure of a superposition turbo encoder based on the structure of [8], [9] for the family of 16-point square constellations, for which examples are illustrated in Figure 2. It is a parallel concatenated TCM with constituent encoder of rate-4/4. In fact, the constituent code consists of two identical recursive convolutional codes of rate-2/2. The rate-2/2 recursive convolutional encoder may be considered as a rate-2/3 recursive convolutional encoder with one systematic bit punctured.

The upper rate-4/4 constituent encoder has as systematic outputs the two most significant input bits (MSBs) while the lower rate-4/4 encoder has as systematic outputs the two least significant input bits (LSBs). Thus the systematic bits are evenly divided between the constituent encoders, and the overall turbo code cannot be catastrophic.

The rate-2/2, 8-state recursive convolutional encoder within the constituent encoders is obtained through exhaustive computer search, and optimized for normalized d_{s2}^E, where d_{s2}^E represents effective free distance. The superscript E refers to the output squared Euclidean distance, and the subscript $s2$ denotes the symbol-wise input weight is two.

According to Fragouli [9], an upper bound on effective free distance for convolutional encoder with multiple "disconnected" shift registers is constrained by the minimum length shift register. Thus, the number of memory elements of two recursive convolutional encoders in the same constituent code should be the same. We found a good rate-4/4 constituent code with identical rate-2/2 recursive convolutional encoders for the two input MSBs and for the two input LSBs. The 8-state recursive convolutional code we found by optimizing normalized d_{s2}^E is

$$A = \begin{bmatrix} 0 & 1 & 0 \\ 0 & 0 & 1 \\ 1 & 1 & 0 \end{bmatrix}, \quad B = \begin{bmatrix} 0 & 0 & 1 \\ 0 & 1 & 1 \end{bmatrix}, \tag{10}$$

$$C = \begin{bmatrix} 1 & 0 \\ 0 & 0 \\ 1 & 0 \end{bmatrix}, \quad D = \begin{bmatrix} 1 & 0 \\ 0 & 1 \end{bmatrix}. \tag{11}$$

in the encoder state-space description:

$$[s_1\ s_2\ s_3]_{j+1} = [s_1\ s_2\ s_3]_j \cdot A + [u_1\ u_2]_j \cdot B \tag{12}$$

$$[y_1\ y_2]_j = [s_1\ s_2\ s_3]_j \cdot C + [u_1\ u_2]_j \cdot D \tag{13}$$

We applied extended spread symbol interleavers [8] to the above constituent code. The extended spread symbol interleaver is a semi-random interleaver due to the random selection without replacement of N integers from 1 to N under certain constraints.

Figure 4 shows the superposition turbo TCM encoder for 8-point circular constellation. Two levels of superposition are used for this structure. A BPSK data stream (i.e. the LSB) is added on top of a QPSK data stream. Since we use rate-1/2 code for the LSB, we encode two 8-PSK symbols at the same time. The rate-2/2 8-state recursive convolutional code described by (10-13) is also used for each sub-code of the constituent code for the 8-point circular constellation encoder.

Our superposition turbo TCM encoder for 64-point square constellation is the direct extension of the encoder in Figure 3. Three levels of superposition are used for this structure. Three QPSK data streams are summed together to generate the transmitted data stream. Again, the code described by (10-13) is used for each sub-code of the constituent code.

B. Decoder

We use two-stage decoding for the two-rate encoder of Figure 3. Figure 5 shows the detailed data flow of the decoder for implementation. It is similar to the "onion peeling" algorithm in [15].

The first decoding stage decodes the two input MSBs. It uses an 8-state-trellis, and calculates the metric by summing up the squared Euclidean distances between the received symbol and all four constellation points of the same quadrant.

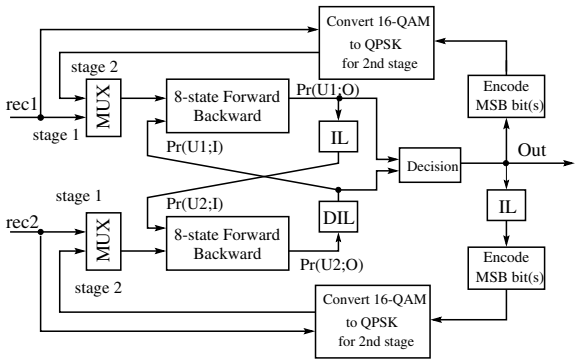

Fig. 5. PCTCM Superposition Turbo TCM Decoder

Before starting the second decoding stage, the received 16-point square constellation symbols are converted to QPSK symbols. The first decoding stage essentially selects a quadrant of the 16-point square constellation. The four points in this quadrant are shifted and possibly reflected about the X or Y axis to produce a noise-distorted point from a QPSK constellation whose labeling is the same regardless of the originating quadrant.

The second decoding stage decodes two input LSBs by decoding the resulting QPSK symbols. The block diagrams of the multi-stage-decoding for the three-rate encoder using a 64-point square constellation and two-rate encoder using a 8-point circular constellation are similar to that for 16-point square constellation in Figure 5. We use a three-stage algorithm for the three-rate decoder, and a two-stage algorithm for the two-rate decoders.

Generally, with the constituent code consisting of multiple independent codes, joint decoding outperforms separately decoding the multiple codes. But, in this degraded broadcast channel, two-stage decoding has essentially the same performance as that of joint decoding. Moreover, the complexity of the joint decoding algorithm is sixteen times that of the two-stage decoding scheme with our specific 16-point square constellation labeling.

For receivers with high SNR, the two input MSBs are effectively error free. Joint decoding with 64-state trellises performs the same as two-stage decoding with 8-state trellises.

For receivers with low SNR, only the first stage of two-stage decoding is conducted. By summing up the squared Euclidean distance between the received symbol and all four constellation points belonging to the same quadrant as the metric, the first decoding stage in fact performs joint decoding of the two MSBs of the 16-QAM symbol.

IV. Simulation Results

This section discusses simulation results for two-rate and three-rate superposition turbo TCM structures with a 16-point square constellation, an 8-point circular constellation and 64-QAM. The interleavers used in the simulations are semi-random interleavers [8]. To describe an interleaver we give the constraint parameters (defined in [8]) in the following order: (S, T, X), where $S_1 = S_2 = S$, $T_1 = T_2 = T$, and $X_1 = X_2 = X$.

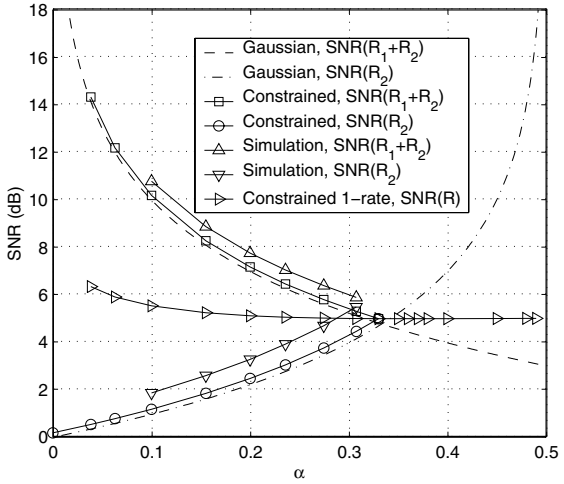

Fig. 6. Error free SNR for high rate and low rate receivers vs. α; interleaver length = 8,192; number of iter. = 15; $BER = 10^{-5}$; $R_1 = R_2 = 1$ (bit/s/Hz); 16-point square constellation

A. Two-rate Superposition with a 16-point Constellation

Figure 6 shows SNR required for $BER = 10^{-5}$ vs. α for the two-rate encoder using a 16-point square constellation. For the various α's from 0.1 to 0.3077 that we simulated, the error free SNR is within 1.0 dB of constrained capacity at BER of 10^{-5}. The symbol interleaver has design parameters $(S = 54, T = 6, X = 1)$ and lengths 8,192. The constituent code searched was optimized for the 16-QAM (i.e. α = 0.2). But, it works fine with other α's. For 16-QAM (α = 0.2), at high and low SNRs, the performance is within 0.6 dB and 1.0 dB of constrained capacity at BER of 10^{-5} respectively.

The first two curves listed in the legend of Figure 6 are theoretical results from (5-6) with fixed rates $R_1 = R_2 = 1$. Both the transmitted signal and noise are assumed to be Gaussian for these two curves. The third and forth curves are numerically calculated constrained capacities, in which the noise is still Gaussian, but the transmitted signals are 16 equi-probable constellation points placed according to α. Curves five and six are the simulation results with various α. The last curve is the numerically calculated constrained capacity for single rate scheme using the 16 constellation points associated with a particular α.

Taking into account that the transmitted signal is not Gaussian, when $\alpha = 0.33015$ (instead of 1/3), the two-rate and single rate schemes should theoretically perform the same. Our simulation results for an α of 0.3077 are as good as that of typical single rate TCM with α of 0.2 [8], [11]. The theoretical performance of the single rate scheme is not sensitive to the change of α for $\alpha \geq 0.2$.

B. Two-rate Superposition with an 8-point Constellation

Figure 7 shows SNR required for $BER = 10^{-5}$ vs. α for a two-rate structure using an 8-point circular constellation. The theoretical range for α is from 0 to $\frac{\sqrt{2}-1}{2\sqrt{2}-1}$ (i.e. 0.2265), under the assumption that both transmitted signal and the noise have Gaussian distributions. Including the performance-loss

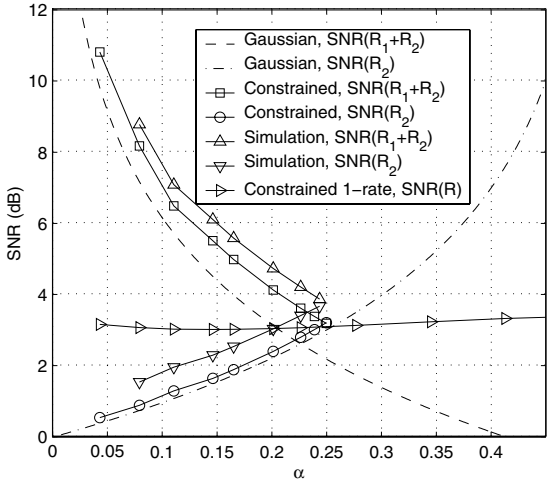

Fig. 7. Error free SNR for high rate and low rate receivers vs. α; interleaver length = 8,192; number of iter. = 15; $BER = 10^{-5}$; $R_1 = R_2 = 1$ (bit/s/Hz); 8-point circular constellation

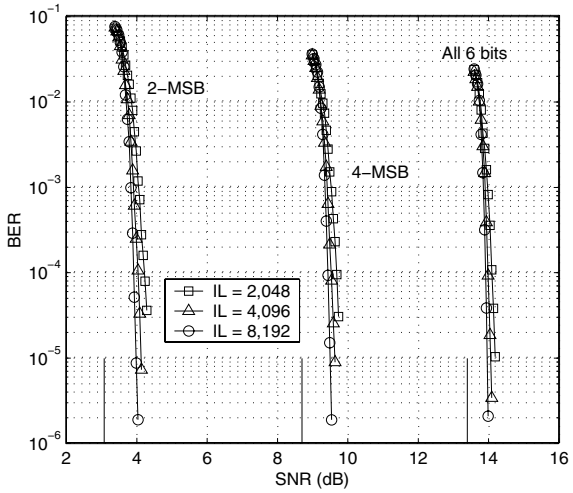

Fig. 8. Three-rate Structure with 64-QAM, Constrained capacities = 3.0913 (dB), 8.7095 (dB) and 13.4094 (dB), 15 iterations

due to an 8-point circular signaling constellation, the practical range of α is around 0 to 0.25. For the various α's from 0.0794 to 0.25 that we simulated, the SNR is within 0.7 dB of constrained capacity at BER of 10^{-5}. The symbol interleaver has design parameters $(S = 54, T = 6, X = 1)$ and length 8,192.

C. Three-rate Superposition with 64-QAM

Figure 8 shows BER vs. SNR for three SNR ranges with $R_1 = R_2 = R_3 = 1$, using 64-QAM ($\alpha_1 = 1/21$, $\alpha_2 = 4/21$), where α_1 and α_2 are the power allocation parameters in (7-8). The constrained capacities are 3.1 dB, 8.7 dB and 13.4 dB for low, middle and high SNR ranges respectively. The interleavers with length of 8,192, 4,096 and 2,048 have constraint parameters $(S = 54, T = 6, X = 1)$, $(S = 37, T = 5, X = 1)$, and $(S = 26, T = 4, X = 0)$ respectively. For 64-QAM at BER of 10^{-5}, the performance is within 0.6, 0.8 and 0.9 dB of constrained capacity at high, middle and low SNR respectively.

In general, for our simulations, the performance at high SNR is closest to the theoretical limit, and the performance at middle SNR is closer than that at low SNR.

V. Conclusion

This paper illustrates that, with turbo codes, superposition coding with multi-stage decoding performs quite well, always within 1 dB of the achievable region boundary. In the context of the work of Cover and Bergmans [2], [4], and the well-known power of turbo codes, this is not that surprising.

Multilevel coding is a special case of multi-rate superposition coding with α selected so that all rates are decoded at the same SNR. The proposed superposition schemes offer the same complexity and performance as that of the typical turbo TCM for this power allocation parameter α, but provide the flexibility of controlling unequal error protection through the choice of α.

VI. Acknowledgments

The first author thanks Chris Jones for the valuable discussions about simulation and Robertson-Wörz turbo TCM structure.

References

[1] T. M. Cover. Broadcast channels. *IEEE Trans. on Info. Theory*, 18(1):2–14, January 1972.

[2] P. P. Bergmans. Random coding theorem for the broadcast channels with degraded components. *IEEE Trans. on Info. Theory*, 19(2):197–207, March 1973.

[3] P. P. Bergmans. A simple converse for broadcast channels with additive white Gaussian noise. *IEEE Trans. on Info. Theory*, 20(2):279–280, March 1974.

[4] T. M. Cover. Comments on broadcast channels. *IEEE Trans. on Info. Theory*, 44(6):2524–2530, October 1998.

[5] L. Wei. Coded modulation with unequal error protection. *IEEE Trans. on Comm.*, 41(10):1439–1449, October 1993.

[6] S. Gadkari and K. Rose. Time-division versus superposition coded modulation schemes for unequal error protection. *IEEE Trans. on Comm.*, 47(3):370–379, March 1999.

[7] X. Wang and M. T. Orchard. Design of superposition coded modulation for unequal protection. In *Proceedings of ICC2001*, pages 4120–416, June 2001.

[8] C. Fragouli and R. D. Wesel. Turbo-encoder design for symbol-interleavered parallel concatenated trellis-coded modulation. *IEEE Trans. on Comm.*, 49(3):425–434, March 2001.

[9] Christina Fragouli. *Turbo Code Design for High Spectral Efficiency*. PhD thesis, University of California at Los Angeles, September 2000.

[10] S. Benedetto and G. Montorsi. Unveiling turbo codes: some results on parallel concatenated coding schemes. *IEEE Trans. on Info. Theory*, 42(2):409–428, March 1996.

[11] P. Robertson and T. Wörz. Bandwidth-efficient Turbo Trellis-Coded Modulation using punctured component codes. *IEEE J. Select. Areas Commun.*, 16(2):206–218, February 1998.

[12] U. Wachsmann, F. H. Fischer, and J. B. Huber. Multilevel codes: theoretical concepts and practical design rules. *IEEE Trans. on Info. Theory*, 45(5):1361–1391, July 1999.

[13] G. Ungerboeck. Channel coding with multilevel/phase signals. *IEEE Trans. on Info. Theory*, 28(1):55–67, January 1982.

[14] R. D. Wesel, X. Liu, J. M. Cioffi, and C. Komninakis. Constellation labeling for linear encoders. *IEEE Trans. on Info. Theory*, 47(6):2417–2431, September 2001.

[15] N. Chayat and S. Shamai. Iterative soft onion peeling for multi-access and broadcast channels. In *Proceedings of 9th International Symposium on Personal, Indoor, and Mobile Radio Communications (PIMRC'98)*, pages 1385–1390, September 1998.